

## NMR evidence for Mott-Hubbard localization in $(\text{NH}_3)\text{K}_3\text{C}_{60}$

H. Tou,<sup>1</sup> Y. Maniwa,<sup>1</sup> Y. Iwasa,<sup>2</sup> H. Shimoda,<sup>2</sup> and T. Mitani<sup>2</sup>

<sup>1</sup>*Department of Physics, Tokyo Metropolitan University, Minami-osawa, Hachi-oji, Tokyo 192-0397, Japan*

<sup>2</sup>*Japan Advanced Institute of Science and Technology, Tatsunokuchi, Ishikawa 923-1292, Japan*

(Received 20 April 2000)

<sup>13</sup>C, <sup>1</sup>H, and <sup>39</sup>K-NMR measurements of  $(\text{NH}_3)\text{K}_3\text{C}_{60}$  unambiguously demonstrated that its magnetic properties are described as a  $S=1/2$  localized spin system over the entire temperature range (300 K–4.2 K). A possible antiferromagnetic structure that appeared below 45 K is compatible with the orientational order of K-NH<sub>3</sub> pairs on the octahedral (O) site. The present NMR study strongly suggests that the Mott-Hubbard localization occurs due to the removal of the C<sub>60</sub>  $t_{1u}$ -orbital degeneracy.

In alkali (A) fullerenes  $A_3\text{C}_{60}$  having face-centered-cubic (fcc) structure, the triply degenerated C<sub>60</sub>  $t_{1u}$  band (e.g.,  $\phi_x$ ,  $\phi_y$ , and  $\phi_z$ ) with half-filling is responsible for the observed metallic and superconducting properties.<sup>1–3</sup> Theoretically, however, a simple argument based on the Mott parameter,  $U/w > 1$ , where  $U$  and  $w$  are the intramolecular Coulomb interaction and the bandwidth, respectively, leads to a Mott-Hubbard localization.<sup>1,2</sup> This paradox was proposed to be solvable by taking into account orbital degeneracy, which increases the critical value for  $U/w$  to 2.5 (Refs. 1 and 4) and/or competition between spin fluctuations and phonon dynamics.<sup>5</sup> In this perspective, the electronic state of trivalent C<sub>60</sub> compounds having distorted structure is interesting, because such distortions may remove the  $t_{1u}$ -orbital degeneracy.

Rosseinsky *et al.* succeeded in preparing  $(\text{NH}_3)\text{K}_3\text{C}_{60}$  having a noncubic structure, and found that the material does not show superconductivity.<sup>6</sup> Further experiments revealed that  $(\text{NH}_3)\text{K}_3\text{C}_{60}$  exhibits a metal-insulator transition at 40 K,<sup>7</sup> at which the low-temperature ( $T$ ) state was believed to be an antiferromagnetic (AF) or a spin-density wave state.<sup>8,9,10</sup> Recently, we reported that the ground state is an AF state of  $1\mu_B/\text{C}_{60}$ . However, the question as to whether the system is insulating had not been resolved.<sup>9</sup> In this paper, we report the NMR results that the magnetic properties of  $(\text{NH}_3)\text{K}_3\text{C}_{60}$  are described as a localized spin system over the entire  $T$  range (300 K–4.2 K).

Sample preparation<sup>7,11</sup> and NMR techniques<sup>3,12</sup> have been reported elsewhere. The crystal structure is a face-centered-orthorhombic (fco) structure, in which K<sub>O</sub>-NH<sub>3</sub> pairs in the O-site (K<sub>O</sub> refers to the O-site potassium) are ordered in an *antiferroelectric* (AFE) fashion at  $T_s \sim 150$  K.<sup>11</sup> NMR spectra at 4.2 K were taken point by point as the frequency was varied. We used a sample having a NH<sub>3</sub> content of 0.98NH<sub>3</sub> per C<sub>60</sub>, which is the same batch as sample A in the x-ray diffraction (XRD) studies.<sup>11</sup> dc-SQUID (superconducting quantum interference device) susceptibility shows anomalies at  $T_s \sim 150$  K and  $T_N \sim 45$  K associated with the AFE and the AF orderings, respectively. We also performed <sup>13</sup>C-NMR for other samples having 1.14NH<sub>3</sub> and 1.05NH<sub>3</sub>. Microscopic examinations revealed that the magnetic character strongly depends on the sample-quality, i.e., NH<sub>3</sub> content. Improvement of the quality and accumulation of experimental data

enabled us to extract intrinsic behaviors. For example, a Curie tail observed at low  $T$ 's in the susceptibility data corresponds to 0.5% spins per C<sub>60</sub> in a well-controlled sample,  $(\text{NH}_3)_{0.98}\text{K}_3\text{C}_{60}$ , which is smaller than 2.6% spins for the previous sample having 1.14NH<sub>3</sub>.<sup>7</sup>

Figures 1 and 2 show the  $T$  dependence of <sup>13</sup>C-NMR spectra and <sup>13</sup>C nuclear spin-lattice relaxation rate,  $1/T_1$ , respectively. Above  $T_s$ , the <sup>13</sup>C line is narrowed by rapid rotation of the C<sub>60</sub> molecules. In this  $T$  region, the susceptibility follows the Curie-Weiss law and yields the effective moment,  $\mu_{eff} \sim 1.746\mu_B/\text{C}_{60}$ , and the Weiss temperature,  $\Theta \sim -160$  K, indicating the total spin “ $S=1/2$ .” Correspondingly,  $1/T_1$  remains constant upon cooling, regardless of the applied magnetic field strength, as expected for a lo-

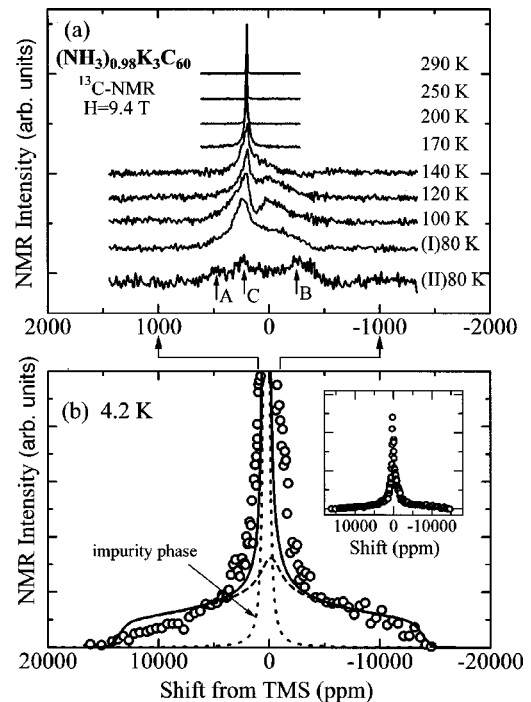


FIG. 1.  $T$  dependence of <sup>13</sup>C-NMR spectra at  $H=9.4$  T (a) above  $T_N$  and (b) at 4.2 K. (I)80 K and (II)80 K show the spectra obtained at different times ( $t=5$  sec and 20 msec, respectively) after saturation of the nuclear magnetization. The dashed line is the calculation for  $\mu_0=1\mu_B/\text{C}_{60}$ , and the solid line is that for a 20%-impurity phase.

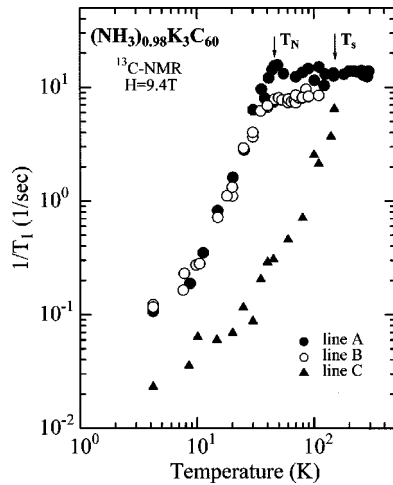


FIG. 2.  $T$  dependence of  $^{13}\text{C}$   $1/T_1$ . Magnetization recovery (MR) above  $T_s$  is fitted by a single exponential function. Below  $T_s$ , the  $1/T_1$ 's are measured for lines A, B, and C.

calized spin system. In this case,  $1/T_1$  is expressed as<sup>13</sup>  $1/T_1 = \sqrt{2\pi}(g\gamma_N)^2(A_{iso}^2 + A_{dip}^2/2)S(S+1)/(3\omega_{ex})$ , where  $\omega_{ex}^2 = 8zJ^2S(S+1)/(3\hbar^2)$  and  $T_N = |J|zS(S+1)/(3k_B)$ ;  $g$ ,  $\gamma_N$ ,  $A_{iso}$ ,  $A_{dip}$ ,  $z$ , and  $J$  are the  $g$  factor, the nuclear gyromagnetic ratio, the isotropic hyperfine coupling constant, the dipolar coupling constant, the number of nearest-neighbor moments, and the exchange constant, respectively. Using  $A_{iso} = 0.326 \text{ kOe}/(\mu_B/C_{60})$ ,<sup>12</sup>  $A_{dip} = 1.58 \text{ kOe}/(\mu_B/C_{60})$ ,<sup>12</sup>  $T_N = 45 \text{ K}$ , and  $S = 1/2$ ,  $1/T_1$  is estimated to be  $13.04 \text{ sec}^{-1}$  for the fcc structure in which  $z = 8$ . This agrees well with the observed value,  $13 \text{ sec}^{-1}$ , implying that a localized model having  $S = 1/2$  is applied to the present system.

Below  $T_s$ , the  $^{13}\text{C}$ -NMR spectrum broadens over the range from  $-500$  to  $+500$  ppm which exceeds the range of  $-100 \sim +400$  ppm for various fullerenes.<sup>2,3,12,14</sup> The spectra “(I)80 K” and “(II)80 K” were taken at different times ( $t = 5$  sec and 20 msec, respectively) after saturation of the nuclear magnetization. The spectrum “(II)80 K” for  $t = 20$  msec splits into several lines (at least more than three) at around 500 ppm (line A),  $-300$  ppm (line B), and 195 ppm (line C), suggesting a hybridization effect, as discussed later. In “(I)80 K” for  $t = 5$  sec, we can see that only line C forms a peak. This indicates that  $T_1$  for line C ( $T_{1C}$ ) is longer than those for lines A and B ( $T_{1A}$  and  $T_{1B}$ , respectively).

In order to avoid mixing of the  $1/T_1$  of line C, which has a large peak intensity, and those of lines A and B, we used a longer rf-pulse width,  $40 \mu\text{sec}$ , for lines A and B than that,  $6 \mu\text{sec}$ , for line C.  $1/T_{1A}$  and  $1/T_{1B}$  were obtained by fitting a stretched exponential function to magnetization recovery (MR) data using parameter  $\alpha \sim 0.8$ . Meanwhile,  $1/T_{1C}$  was tentatively determined by fitting  $M_C(t) = M_0[1 - S_{AB}\exp(-t/T_{1A}) - S_C\exp(-t/T_{1C})]$  to MR data. For  $T_s > T > T_N$ ,  $S_{AB}/S_C \sim 0.8/0.2$  is obtained, suggesting the intensity of the line C is 20% for the entire range. For  $T < T_N$ ,  $S_{AB}/S_C \sim 0.2/0.8$  because of a wipeout effect due to a magnetic ordering.

$1/T_{1C}$  shows a remarkable drop by an order just below  $T_s$  and is nearly proportional to  $T$  down to 4.2 K, without any anomaly at  $T_N$ . In the sample having  $1.14\text{NH}_3$ , neither the spectral splitting related to lines A and B below  $T_s$  nor the

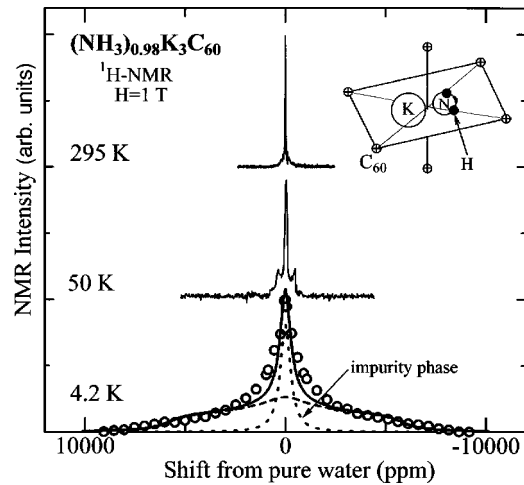


FIG. 3.  $T$  dependence of  $^1\text{H}$ -NMR spectra. The dashed line is the calculation for  $\mu_0 = 1\mu_B/C_{60}$ , and the solid line is that for 20%-impurity phase. Here, the calculated line was convoluted by a computed spectrum using the Lorentzian fit to the 50 K spectrum. The inset shows the local symmetry of the octahedral site below  $T_s$ .

magnetic spectral broadening below  $T_N$  were observed.<sup>7</sup> Thus, lines A and B are inherent in the AF ordering, whereas line C originates in the impurity phase. This also implies that the electronic state is very sensitive to the  $\text{NH}_3$  content and that off-stoichiometric ammoniation leads to imperfect AFE and AF ordering.

In contrast, both  $1/T_{1A}$  and  $1/T_{1B}$  remain constant upon cooling through  $T_s$ , suggesting that the local moment picture is maintained. This implies that the averaged effective exchange frequency due to nearest-neighbor  $\text{C}_{60}$  spins does not change through  $T_s$ . The difference between  $1/T_{1A}$  and  $1/T_{1B}$  may instead be attributed to that of the hyperfine coupling constant.

Below  $T_N \sim 45 \text{ K}$ , the  $^{13}\text{C}$  NMR spectrum is unusually broadened around a narrow center line [see Fig. 1(b)]; the width is about 27 000 ppm ( $\sim 2.7 \text{ MHz}$ ) at 4.2 K, which indicates the AF order. Since the line broadening is mainly attributed to on-site dipolar hyperfine interactions with the local spin density at the carbon  $2p_z$  orbital, we can deduce the dipolar field due to the spin density as  $H_{2p_z} = -0.6\langle 1/r^3 \rangle_{2p_z} \mu_{2p_z} \cos \alpha \sin \beta \cos \beta$ , and  $\mu_{2p_z} = \mu_0/60$ .  $\mu_0$  is defined as the magnitude of the magnetic moment per  $\text{C}_{60}$ , and  $\alpha$  and  $\beta$  are the polar angles between the applied magnetic field  $\vec{H}$  and the carbon  $2p_z$  orbital. Here, we assume the spin-flop phase of the AF ordered state,  $\vec{\mu}_0 \perp \vec{H}$ .<sup>15,16</sup> The line width is estimated to be  $\Delta f \sim 2.4 \text{ MHz}/(\mu_B/C_{60})$  ( $\sim 24 \text{ 000 ppm}$ ) using  $\langle 1/r^3 \rangle_{2p_z} \sim 1.89/a_B^3$ , where  $a_B$  is the Bohr radius.<sup>12</sup> We found that the observed spectrum can be reproduced by the calculation using  $\mu_0 = 1\mu_B/C_{60}$  and the 20%-impurity phase, as shown in Fig. 1(b).

Figures 3 and 4 display NMR spectra for  $^1\text{H}$  and tetrahedral site potassium ( $^{39}\text{K}$ ),<sup>17</sup> respectively. Below  $T_s$ , the  $^{39}\text{K}$  NMR shows the isotropic positive shift of  $+200$  ppm with spectral broadening to be different from that of  $\text{K}_3\text{C}_{60}$ ,<sup>18</sup> whereas the  $^1\text{H}$  NMR does not show any anomaly

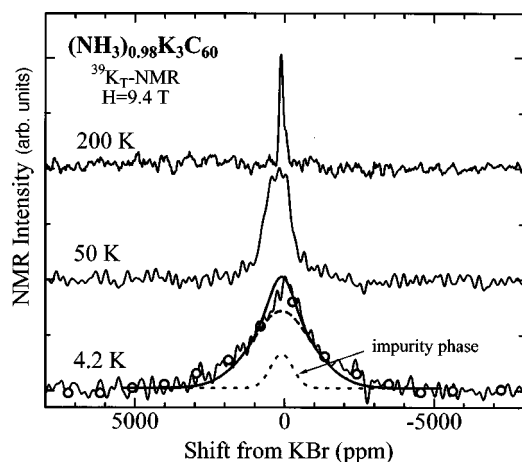


FIG. 4.  $T$  dependence of  $^{39}\text{K}$ -NMR spectra. The dashed line is the calculation for  $\mu_0 = 1 \mu_B / C_{60}$ , and the solid line is that for the 20%-impurity phase. Here, the calculated line was convoluted by a computed spectrum using the Gaussian fit to the 50 K spectrum.

lies. These findings suggest that the  $C_{60}$  hybridizes with the  $K_O$  orbital rather than the H orbital, as expected from the XRD studies.<sup>11</sup>

Below  $T_N$ ,  $^1\text{H}$ - and  $^{39}\text{K}_T$ -NMR spectra<sup>19</sup> also show line broadening. The  $^1\text{H}$ - and  $^{39}\text{K}_T$ -NMR provide information on the AF ordering vector through the local field,  $\vec{H}_{\parallel}^{loc} = \sum_i [3(\vec{\mu}_{0i} \cdot \vec{r}_i) \vec{r}_i / r_i^5 - \vec{\mu}_{0i} / r_i^3]_{\parallel}$ , where  $\vec{r}_i$  is the position of  $i$ th  $C_{60}$  molecule and the notation “ $\parallel$ ” represents the component of  $\vec{H}^{loc} \parallel \vec{H}$ . For simplicity, any helical or noncollinear magnetic structure was disregarded and we confined ourselves to perform calculations only for the AF structures with ordering vectors,  $\vec{Q} = (0 \ 0 \ 2)$ ,  $(1 \ 1 \ 1)$ ,  $(1 \ 2 \ 0)$ ,  $(2 \ 2 \ 1)$ , and  $(2 \ 2 \ 0)$  with respect to the low  $T$  fcc unit cell. These structures are deduced from the mean-field theory and the former three  $\vec{Q}$ 's correspond to type I, II, and III fcc AF structures, respectively, whereas the latter two correspond to the body-centered-tetragonal AF structures with  $\vec{Q} = (1/2 \ 1/2 \ 1/2)$  and  $(1/2 \ 1/2 \ 0)$ , respectively.<sup>20</sup> The calculations were performed for the spin-flop phase with  $\mu_0 = 1 \mu_B / C_{60}$ , and the sum runs over neighbor  $C_{60}$ 's of  $^{39}\text{K}_T$  ( $i = 1$  to 4) and  $^1\text{H}$  ( $i = 1$  to 6). The position of hydrogen is averaged over the 1D  $\text{NH}_3$  molecular rotation.<sup>21</sup> As shown in Figs. 3 and 4, good agreements with the observed spectra are obtained for a 3D-AF structure so as to satisfy the 3D-AFE order where 2D-AF sheets with planer ordering vectors of  $\vec{q}_{2D}^+ = (1 \ 1)$  and  $\vec{q}_{2D}^- = (-1 \ 1)$  are stacked alternately along the  $c$  axis: other  $\vec{Q}$ 's yield 1.7–3.5 times as broad linewidth as the observed  $^1\text{H}$ -NMR width. Here, the 20%-impurity phase was taken into account. Figure 5 shows the obtained AF structure, in which black and white rugby balls correspond to opposite spins. Here we note that the AF structure is not the simple  $\vec{Q}$ , but rather the complicated  $\vec{Q}$  that is well correlated with the AFE structure. This suggests that the  $K_O$ - $\text{NH}_3$  arrangement within the  $ab$  plane plays an important role in the AF ordering.

Next, we discuss the ground state of the system. The present result satisfies the Rhodes-Wohlfarth relation of  $\mu_C / \mu_0 \sim 1$ , where  $\mu_C = (1 + \mu_{eff}^2)^{0.5} - 1$ , for the localized

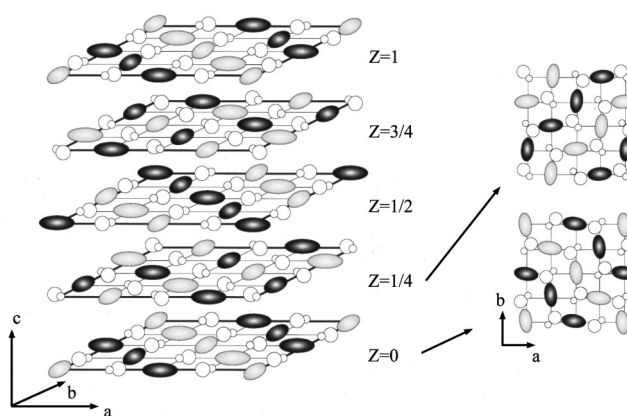


FIG. 5. Proposed AF structure and *molecular orbital order*. Rugby balls and open large and small balls represent  $\phi_x$  or  $\phi_y$  of the  $C_{60} t_{1u}$  orbitals, K and  $\text{NH}_3$ , respectively. Black and white rugby balls correspond to opposite spins. For simplicity,  $K_T$  atoms are not shown.

electron system.<sup>22</sup> In itinerant electron magnets, however, the total spin usually shrinks in the ordered state, i.e.,  $\mu_C / \mu_0 > 1$ .<sup>22</sup> Thus,  $(\text{NH}_3)\text{K}_3\text{C}_{60}$  is described as a localized electron system having a low-spin (LS) configuration of  $S = 1/2$  over the entire  $T$  range, strongly suggesting that the stoichiometric  $(\text{NH}_3)\text{K}_3\text{C}_{60}$  is a *Mott-Hubbard insulator*.

Why does the Mott-Hubbard localization take place? The lattice expansion and the distortion from a cubic structure seem insufficient to induce the localization, because both fcc  $\text{A}_3\text{C}_{60}$ 's having almost the same cell volume and  $\text{Cs}_3\text{C}_{60}$  having a distortion are not insulators.<sup>2,3,11</sup> A possible origin is the symmetry breaking at  $C_{60}$  sites due to an interaction with the  $K_O$ - $\text{NH}_3$  pairs. This would remove the  $t_{1u}$  degeneracy due to a Jahn-Teller effect<sup>23</sup> assisted by an asymmetric crystal field and lead to the Mott-Hubbard localization.<sup>1,4</sup> The  $^{13}\text{C}$  and  $^{39}\text{K}_T$  NMR spectra indicate that the interaction between  $C_{60}$  and  $K_O$  ions, which lowers the local symmetry at  $C_{60}$  site, is more substantial than that in fcc  $\text{A}_3\text{C}_{60}$ 's: the broader  $^{13}\text{C}$  spectra and the larger shift of  $^{39}\text{K}_T$  spectra at low  $T$ .

Furthermore, such a strong interaction between the  $t_{1u}$  band and the pairs may cause the  $t_{1u}$  orbitals order at  $T_s$ . This is a kind of *molecular orbital order* of  $\phi_x$  and  $\phi_y$ , as shown by the rugby balls in Fig. 5. Thus the close relationship between the AF and the AFE order is considered to be a natural consequence of the molecular orbital order; the black (white) rugby balls couple each other through the  $K_O$  atoms, whereas there is no  $K_O$  between the black and white rugby balls in the  $ab$  plane.

Theoretical investigations have suggested that the degenerated  $t_{1u}$  level is unstable for the trivalent  $C_{60}$  and may be split into three levels in the LS configuration<sup>23</sup> due to a strong electron-phonon interaction, i.e., the Jahn-Teller effect.<sup>5</sup> In the present case, the Jahn-Teller distortion and band splitting are realized by the aid of the interaction between  $K_O$  ion and the  $t_{1u}$  orbital. Thus, the AFE order causes the molecular orbital ordering and the AF ordering. The coupling between the  $t_{1u}$  band and the  $K_O$ - $\text{NH}_3$  pairs must be responsible for the realization of the AF ground state. This is

consistent with the result that the imperfect AFE ordering prevents the AF order, as mentioned earlier.

In conclusion,  $^{13}\text{C}$ ,  $^1\text{H}$ , and  $^{39}\text{K}$ -NMR studies have provided evidence that  $(\text{NH}_3)\text{K}_3\text{C}_{60}$  is the  $S = 1/2$  localized spin system and strongly suggested that the ground state is a Mott-Hubbard AF insulator having  $\mu_0 \sim 1 \mu_B / \text{C}_{60}$ . The previously observed metallic behaviors are probably due to the imperfect AFE and molecular orbital ordering. We propose that the magnetic structure is the 3D AF order correlated with the AFE arrangement and is accompanied by the *molecular orbital order*. The present study established that the

electronic state of the fcc  $\text{A}_3\text{C}_{60}$  is close to the Mott-Hubbard localization and is sensitive to the local symmetry at  $\text{C}_{60}$  site.

The authors gratefully acknowledge K. Ishii, S. Suzuki, H. Suematsu, and F. Simon for their valuable discussions. H.T. would like to thank H. Ikeda and T. Hotta for their useful comments. This work was supported in part by Grants from the Ministry of Education, Sport, Science and Culture in Japan, by Priority Areas Grants of the "Fullerene and Nanotube," by the Fund for Special Research Projects of Tokyo Metropolitan University, and by the JSPS "Future Program" (RFTF96P00104).

- 
- <sup>1</sup>O. Gunnarsson, Rev. Mod. Phys. **69**, 575 (1997).
  - <sup>2</sup>C.H. Pennington and V.A. Stenger, Rev. Mod. Phys. **68**, 855 (1996).
  - <sup>3</sup>Y. Maniwa *et al.*, Phys. Rev. B **54**, R6861 (1996).
  - <sup>4</sup>J.P. Lu, Phys. Rev. B **49**, 5687 (1994).
  - <sup>5</sup>S. Suzuki and K. Nakao, Phys. Rev. B **52**, 14 206 (1995).
  - <sup>6</sup>M.J. Rosseinsky *et al.*, Nature (London) **364**, 425 (1993).
  - <sup>7</sup>Y. Iwasa *et al.*, Phys. Rev. B **53**, R8836 (1996).
  - <sup>8</sup>L.M. Allen *et al.*, J. Mater. Chem. **6**, 1445 (1996); K. Prassides *et al.*, J. Am. Chem. Soc. **121**, 11 227 (1999).
  - <sup>9</sup>H. Tou *et al.*, Physica B **259-261**, 868 (1999).
  - <sup>10</sup>F. Simon *et al.*, Phys. Rev. B **61**, R3826 (2000).
  - <sup>11</sup>K. Ishii *et al.*, Phys. Rev. B **59**, 3956 (1999).
  - <sup>12</sup>N. Sato *et al.*, Phys. Rev. B **58**, 12 433 (1998).
  - <sup>13</sup>T. Moriya, Prog. Theor. Phys. **16**, 23 (1956); **16**, 641 (1956).
  - <sup>14</sup>R. Tycko, J. Phys. Chem. Solids **54**, 1713 (1993); M. Mehring *et al.*, Philos. Mag. B **70**, 787 (1994).
  - <sup>15</sup>V. Brouet *et al.*, Phys. Rev. Lett. **76**, 3638 (1996).
  - <sup>16</sup>A. Jánossy *et al.*, Phys. Rev. Lett. **79**, 2718 (1997).
  - <sup>17</sup>N. Muroga *et al.* (unpublished); The present  $^{39}\text{K}$ -NMR spectrum is due to the  $\text{K}_T$  site, on the analogy of  $(\text{NH}_3)_{0.55}\text{NaRb}_2\text{C}_{60}$ , where any O site  $^{23}\text{Na}$ -NMR signal cannot be observed because of the electric field gradient.
  - <sup>18</sup>Y. Yoshinari *et al.*, Phys. Rev. B **54**, 6155 (1996).
  - <sup>19</sup>The quadrupole effect is negligible on the analogy of  $(\text{NH}_3)_{0.55}\text{NaRb}_2\text{C}_{60}$  (Ref. 16) and  $\text{Na}_2\text{CsC}_{60}$  [T. Saito *et al.*, J. Phys. Soc. Jpn. **64**, 4513 (1995)].
  - <sup>20</sup>J.S. Smart, *Effective Field Theory of Magnetism* (W.B. Saunders Co., Philadelphia, 1966); A. Yoshimori, J. Phys. Soc. Jpn. **14**, 807 (1959).
  - <sup>21</sup>Y. Maniwa *et al.*, Synth. Met. **103**, 2458 (1999).
  - <sup>22</sup>P. Rhodes and E.P. Wohlfarth, Proc. R. Soc. London, Ser. A **273**, 247 (1963); T. Moriya and H. Hasegawa, J. Phys. Soc. Jpn. **48**, 1490 (1980).
  - <sup>23</sup>M.S. Dresselhaus, G. Dresselhaus, and P.C. Eklund, *Science of Fullerenes and Carbon Nanotubes* (Academic Press, New York, 1996).